Is the Large Uncertainty of δ_{CP} Fundamentally Encoded in the Neutrino Quantum State?

Michela Ignoti,[1,2,*] Claudia Frugiuele,[2,†] Matteo G. A. Paris,[1,2,‡] and Marco G. Genoni[1,2,§]
[1]*Dipartimento di Fisica "Aldo Pontremoli," Università degli Studi di Milano, I-20133 Milano, Italia*
[2]*INFN Sezione di Milano, I-20133 Milano, Italia*

(Received 10 December 2025; revised 16 January 2026; accepted 19 October 2026; published 12 November 2026)

The precise measurement of the leptonic *CP*-violating phase δ_{CP} remains one of the major open challenges in neutrino physics, as current experiments achieve only very limited accuracy. We address this issue through the lens of quantum estimation theory. A distinctive feature of neutrino oscillation experiments is that they cannot freely optimize the probe or measurement, since both are constrained by the production and detection of flavor eigenstates. We therefore examine whether the large uncertainty in δ_{CP} originates from intrinsic properties—either of the neutrino quantum state or of flavor measurements—or if it instead stems from experimental limitations. By comparing quantum and classical Fisher information, we demonstrate that the limited sensitivity to δ_{CP} originates primarily from the information content of flavor measurements. Furthermore, we show that, while targeting the second oscillation maximum, as in the ESSνSB proposal, typically enhances δ_{CP} information, this feature in fact strongly depends on the actual values of δ_{CP}.

DOI: 10.1103/dgdr-mx1d

Introduction—Neutrinos are among the most elusive particles in nature, interacting only via the weak force. Although the standard model predicts them to be massless, the observation of neutrino oscillations demonstrates that they possess nonzero masses. These oscillations are described by the Pontecorvo-Maki-Nakagawa-Sakata (PMNS) matrix, parameterized by three mixing angles (θ_{12}, θ_{13}, θ_{23}) and a Dirac *CP*-violating phase δ_{CP}. While the mixing angles and mass-squared differences (Δm^2_{21}, Δm^2_{31}) are now determined with percent-level precision, δ_{CP} remains poorly constrained. The NuFIT v6.0 global analysis reports [1], for the normal ordering (NO) scenario, $\delta_{CP}^{(\mathrm{NO})} = 177^{\circ}{}^{+19^{\circ}}_{-20^{\circ}}$, based primarily on data from the long-baseline accelerator experiments T2K [2] and NOνA [3], which produce intense neutrino beams from proton collisions and measure their flavor composition after propagation over hundreds of kilometers. The precision on δ_{CP} remains substantially lower than that of the other mixing parameters, for example, the mixing angle $\theta_{13} = 8.52^{\circ}{}^{+0.11^{\circ}}_{-0.11^{\circ}}$, highlighting the current experimental challenges in probing *CP* violation in the neutrino sector. Next-generation facilities such as DUNE [4,5], T2HK [5–7], and ESSνSB [8,9] aim to significantly improve this precision and may provide the first definitive evidence of leptonic *CP* violation. A nonzero Dirac *CP*-violating phase δ_{CP} in the PMNS matrix would signal *CP* violation in the lepton sector, a key ingredient for leptogenesis [10], and thus supports scenarios connecting low-energy neutrino parameters to high-energy dynamics. Consequently, understanding the origin of the present uncertainty is not merely a technical matter; it is a fundamental inquiry with broad implications for particle physics and cosmology. In this Letter, we address a critical new question: whether the poor determination of the leptonic *CP* phase δ_{CP} arises from intrinsic quantum limits of the neutrino state or from the flavor-based measurements employed in oscillation experiments. Quantum estimation theory (QET) [11,12] provides a rigorous framework to approach this challenge from both a fundamental and practical level. Given a quantum state $|\psi_\lambda\rangle$ that depends parametrically on a parameter λ to be estimated, suppose we perform a quantum measurement described by a set of orthogonal projectors $\{\Pi_x\}$. (Note that in the most general scenario one should consider a set of operators forming a positive-operator valued measure—POVM—but for the scope of this Letter we can restrict to standard projectors.) The variance of any unbiased estimator of the parameter $\tilde{\lambda}$ is lower bounded by the Cramér-Rao bound (CRB)

$$\mathrm{Var}_{\tilde{\lambda}}(\lambda) \geq \frac{1}{MF(\lambda)}. \tag{1}$$

Here M corresponds to the number of independent measurements, while

*Contact author: michela.ignoti@studenti.unimi.it
†Contact author: claudia.frugiuele@mi.infn.it
‡Contact author: matteo.paris@fisica.unimi.it
§Contact author: marco.genoni@unimi.it

Published by the American Physical Society under the terms of the Creative Commons Attribution 4.0 International license. Further distribution of this work must maintain attribution to the author(s) and the published article's title, journal citation, and DOI. Funded by SCOAP³.

$$F(\lambda) = \sum_x \frac{(\partial_\lambda p(x|\lambda))^2}{p(x|\lambda)}, \tag{2}$$

denotes the (classical) Fisher information (FI), written in terms of the conditional probability $p(x|\lambda) = \langle\psi_\lambda|\Pi_x|\psi_\lambda\rangle$. The FI clearly depends on both the state $|\psi_\lambda\rangle$ and on the operators $\{\Pi_x\}$ describing the measurement strategy. Remarkably one can optimize over all the possible measurement operators, and obtain a measurement-independent quantity. In turn, the quantum Fisher information (QFI), defined as $H(\lambda) = \max_{\{\Pi_x\}} F(\lambda)$, is given by

$$H(\lambda) = 4[\langle\partial_\lambda\psi_\lambda|\partial_\lambda\psi_\lambda\rangle - |\langle\partial_\lambda\psi_\lambda|\psi_\lambda\rangle|^2]. \tag{3}$$

As it is apparent from its definition, the QFI sets a more fundamental bound, the so-called quantum Cramér-Rao bound (QCRB)

$$\mathrm{Var}_{\tilde{\lambda}}(\lambda) \geq \frac{1}{MF(\lambda)} \geq \frac{1}{MH(\lambda)}, \tag{4}$$

which ultimately depends only on the quantum state $|\psi_\lambda\rangle$, and not on the particular measurement strategy implemented. Comparisons between the FI and QFI are therefore instructive: if they coincide, the precision limit is intrinsic; if a significant gap exists, the measurement strategy is suboptimal. Standard QET applications focus on designing optimal probes and measurements that optimize and saturate the quantum Cramér-Rao bound, thereby achieving the ultimate precision allowed by quantum mechanics. These approaches have been instrumental in conceiving and assessing quantum sensing protocols that promise a quantum enhancement in the estimation of physical parameters [13–17]. Tools from QET have been employed in high energy physics, for example in the context of the anti–de Sitter/conformal field theory (AdS/CFT) correspondence [18–24], or to assess an Unruh-DeWitt detector [25], universal gravity corrections [26], equivalence principle [27], and gravitational time dilation [28]. More recently, they have been exploited to derive and discuss the ultimate limits on the precision of physical parameters describing a QED scattering experiment [29] and cosmological parameters [30].

This Letter, together with an upcoming paper applying QET to all relevant neutrino oscillation parameters [31], aims to provide a quantitative framework for assessing precision limits in the estimation of the CP-violating phase δ_{CP}, and guiding the design of future experiments.

Unlike typical quantum metrology protocols, neutrino oscillation experiments operate in a fundamentally different regime: neither the probe nor the measurement can be optimized, as both are fixed by the flavor production and detection processes. This constraint implies that intrinsic precision limits may arise from both the quantum state and the measurement. In this context, the central question is not how to engineer optimal settings, but what precision is fundamentally attainable under unavoidable constraints in the design of the estimation protocol. In particular, we investigate whether the restriction to flavor measurements imposes an additional limitation, beyond the intrinsic quantum bound, on the estimation of δ_{CP}.

Since we address the CP-violating phase δ_{CP}, we focus our attention to accelerator-based experiments. To evaluate the impact of the restriction to flavor states and flavor measurements, we work under a set of simplifying assumptions. We consider neutrinos propagating in vacuum and model their quantum states as pure plane-wave states [32–35]. This restriction further limits our Letter to experiments where matter effects are negligible, such as T2K, T2HK [2,36], and the proposed ESSνSB [8,9], and we also assume a monochromatic neutrino beam at its peak energy E, which constitutes a reasonable approximation for these setups.

Under these assumptions, a neutrino produced at time $t_0 = 0$ in a flavor eigenstate $|\nu_\alpha\rangle$ evolves into $|\nu_\alpha(t)\rangle$ at time t, yielding the transition probabilities $P(|\nu_\alpha\rangle \to |\nu_\beta\rangle) = |\langle\nu_\beta|\nu_\alpha(t)\rangle|^2$. The corresponding expressions for antineutrinos, $|\bar{\nu}_\alpha(t)\rangle$ and $P(|\bar{\nu}_\alpha\rangle \to |\bar{\nu}_\beta\rangle)$, are obtained analogously. Further details on these, which form the basis of our analysis, are provided in the End Matter. In general, these quantities will depend on the parameters entering in the PMNS matrix, the squared mass differences $\Delta m^2_{ji} = m^2_j - m^2_i$ of mass eigenstates, and on the ratio L/E between the accelerator baseline L and the beam peak energy E. As we are interested in the precision bounds on δ_{CP}, we will consider all the other parameters fixed according to the NuFIT best values [1] [as regards the mass differences, we focus on the normal mass ordering (NO), but our results are practically identical for the inverted ordering (IO)]. In particular we will then consider the behavior of the corresponding QFIs and FIs as a function of the ratio L/E, as it allows us to properly identify the performances of the different current and future accelerator experiments designed to estimate δ_{CP}.

Evaluating the QCRB—The CP-violating phase is not directly measurable and its value is inferred from flavor-dependent detection rates determined by the oscillation pattern of neutrino propagation. We here proceed to derive the fundamental limits on its estimation precision by evaluating the QFIs corresponding to experiments based on both initial muon-neutrino and muon-antineutrino beams. This can be directly evaluated via Eq. (3) by considering $\lambda = \delta_{CP}$ as the parameter we want to estimate, and by replacing $|\psi_\lambda\rangle$ with either $|\nu_\mu(t)\rangle$ and $|\bar{\nu}_\mu(t)\rangle$. We denote, respectively, with $H_\nu(\delta_{CP})$ and $H_{\bar{\nu}}(\delta_{CP})$ the corresponding QFIs. As neutrino and antineutrino experiments are statistically independent, the ultimate bound on the estimator variance $\mathrm{Var}_{\tilde{\delta}_{CP}}(\delta_{CP})$ in Eq. (4), taking into account both beams, is obtained by replacing the denominator with

$$MH_{\nu,\bar{\nu}}(\delta_{CP}) = M[\xi_\nu H_\nu(\delta_{CP}) + \xi_{\bar{\nu}} H_{\bar{\nu}}(\delta_{CP})], \quad (5)$$

where $\xi_\nu = M_\nu/M$ and $\xi_{\bar{\nu}} = M_{\bar{\nu}}/M$ are, respectively, the fractions of the total number of measurements $M = M_\nu + M_{\bar{\nu}}$ corresponding to either neutrino (M_ν) or antineutrino ($M_{\bar{\nu}}$) events. Our calculations show that, in the parameter regime of interest, $H_\nu(\delta_{CP})$ is approximately equal to $H_{\bar{\nu}}(\delta_{CP})$ (see End Matter for more details). Consequently, we can safely quantify the information contained both in neutrino and antineutrino quantum states simply as the average of the individual QFIs: $H_{\nu,\bar{\nu}}(\delta_{CP}) = [H_\nu(\delta_{CP}) + H_{\bar{\nu}}(\delta_{CP})]/2$. We remark that the total number of events M corresponds to the so-called nonoscillated (anti)neutrinos, that is the total number of events in absence of oscillation phenomena, formally obtained by assuming that the PMNS matrix is the identity, and experimentally efficiently estimated from the number of events obtained at the near detector.

We find that $H_{\nu,\bar{\nu}}(\delta_{CP})$ exhibits no significant dependence on δ_{CP}, indicating that the information content of the quantum state is largely insensitive to the true value of the parameter (see End Matter for more details). Figure 1 shows the QFI for δ_{CP}, evaluated at the NuFIT best-fit value $\delta_{CP}^{(\mathrm{NO})}$: we observe that the QFI peaks remain stable under variations in L/E, demonstrating consistent sensitivity across oscillation maxima. These peaks coincide with the oscillation maxima of $P[\nu_\mu(\bar{\nu}_\mu) \to \nu_e(\bar{\nu}_e)]$, as the highest appearance probability provides maximal information on δ_{CP}. Both T2K and ESSνSB operate near the QFI maximum, making them equally well suited for δ_{CP} measurement from the standpoint of the quantum state's information content. From the corresponding QCRB, we obtain a fundamental limit on the achievable precision of the CP-violating phase: for a total data sample of $M = \mathcal{O}(10^3)$ neutrino and antineutrino events, representing a conservative estimate of current statistics, the corresponding QFI yields a lower bound of approximately 3° on the uncertainty of δ_{CP}. If we take the current best-fit value $\delta_{CP}^{(\mathrm{NO})}$, the resulting uncertainty is at the few-percent level, indicating that the neutrino quantum state intrinsically encodes sufficient information to allow precision measurements even with present-day event statistics.

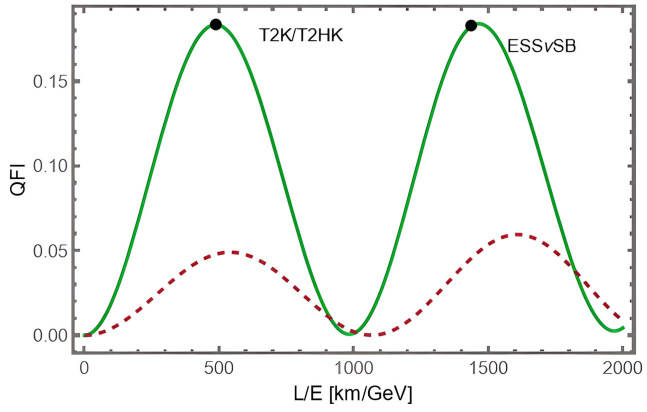


FIG. 1. The effective QFI $H_{\nu,\bar{\nu}}(\delta_{CP})$ (green solid line) and the neutrino appearance probabilities $P(\nu_\mu \to \nu_e)$ (dashed bordeaux line) plotted as a function of L/E and for $\delta_{CP} = \delta_{CP}^{(\mathrm{NO})}$. The two black points correspond to the value of the QFI for the experiments T2K/T2HK and ESSνSB, identified by considering the peak energy E of the neutrino spectrum.

Evaluating the CRB for flavor measurement—The QFI establishes the ultimate quantum limit for parameter estimation; an optimal POVM can always be identified such that the corresponding FI saturates this bound. A detailed discussion on the construction of these optimal measurements is provided in the next section. However, in current neutrino oscillation experiments, the available measurement basis is fundamentally restricted to projections onto flavor eigenstates. In the following, we evaluate the classical FI associated with these flavor-projections via Eq. (2) and analyze its behavior relative to the quantum limit. We define the projectors onto the flavor eigenstates as

$$\Pi_e = |\nu_e\rangle\langle\nu_e| \quad (6)$$

$$\Pi_\mu = |\nu_\mu\rangle\langle\nu_\mu| \quad (7)$$

$$\Pi_{\mathrm{off}} = \mathbb{I} - \Pi_e - \Pi_\mu = |\nu_\tau\rangle\langle\nu_\tau|, \quad (8)$$

where Π_e and Π_μ project onto the electron and muon neutrino states, respectively, and Π_{off} accounts for all outcomes other than ν_e or ν_μ. As we are here assuming that the efficiencies in the detection of both electron and muon neutrinos are equal to one, the last operator does in fact correspond to the detection of tau neutrinos ν_τ. Although ν_τ cannot always be directly detected, its information is still contained in the electron and muon neutrino detections: given the number of muonic and electronic neutrinos detected, M_μ and M_e, the number of tauonic neutrinos can in fact be inferred as $M_\tau = M - (M_\mu + M_e)$; as we mentioned before, the total number of neutrinos M arriving at the far detector of the experiment can be indeed efficiently estimated from the number of events obtained at the near detector [37,38]. An analogous construction applies for a $\bar{\nu}_\mu$ beam, using projectors onto antineutrino flavor eigenstates.

As before, by exploiting the formula in Eq. (2) we can evaluate the FIs corresponding to both neutrino experiments, $F_\nu(\delta_{CP})$, and antineutrino experiments, $F_{\bar{\nu}}(\delta_{CP})$. In this case one can verify that the corresponding values may have a non-negligible difference in some regimes, in particular for values of δ_{CP} corresponding to maximum CP violation. However, it is still true that the two quantities are approximately equal for values of L/E corresponding to probability oscillation maxima, that is, within the regimes probed by current and future neutrino

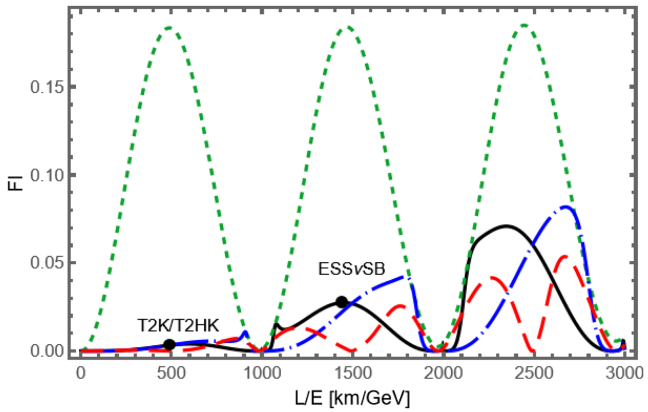


FIG. 2. Classical effective FI corresponding to flavor detection $F_{\nu,\bar{\nu}}(\delta_{CP})$ as a function of the effective baseline L/E and for different values of δ_{CP}: black solid line, $\delta_{CP} = \delta_{CP}^{(\mathrm{NO})}$; red long-dashed line, $\delta_{CP} = \pi/2$; blue dash-dotted line, $\delta_{CP} = 0$. The short-dashed green line corresponds to the effective QFI $H_{\nu,\bar{\nu}}(\delta_{CP})$, while the two black points correspond to the value of the FI for the experiments T2K/T2HK and ESSνSB. These have been identified by considering the peak energy E of the neutrino spectrum.

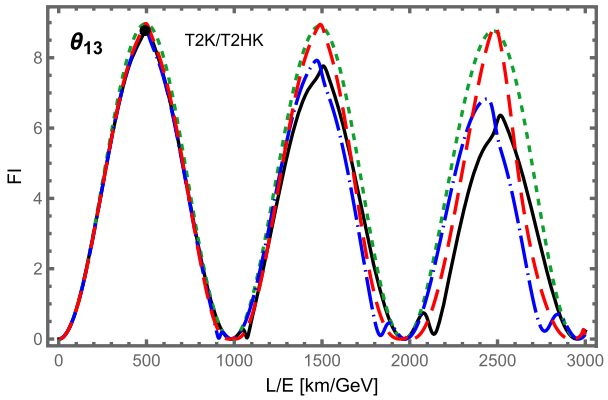


FIG. 3. Classical effective FI corresponding to flavor detection $F_{\nu,\bar{\nu}}(\theta_{13})$ as a function of the effective baseline L/E and for different values of δ_{CP}: black solid line, $\delta_{CP} = \delta_{CP}^{(\mathrm{NO})}$; red long-dashed line, $\delta_{CP} = \pi/2$; blue dash-dotted line, $\delta_{CP} = 0$. The short-dashed green line corresponds to the effective QFI $H_{\nu,\bar{\nu}}(\theta_{13})$, while the black point corresponds to the value of the FI for the experiments T2K/T2HK. These have been identified by considering the peak energy E of the neutrino spectrum.

experiments. We can thus define an effective FI that takes into account both neutrino and antineutrino events as $F_{\nu,\bar{\nu}}(\delta_{CP}) = [F_{\nu}(\delta_{CP}) + F_{\bar{\nu}}(\delta_{CP})]/2$.

In Fig. 2, this quantity is seen to depend on both δ_{CP} and on the location of the maxima, in contrast to the QFI. As required by Eq. (4), the FI never exceeds the QFI: for all δ_{CP} values, $F_{\nu,\bar{\nu}}(\delta_{CP})$ remains below the peaks of $H_{\nu,\bar{\nu}}(\delta_{CP})$, indicating that flavor measurements are suboptimal for estimating δ_{CP} and that the achievable precision is therefore limited by $F_{\nu,\bar{\nu}}(\delta_{CP})$. This behavior is a specific and distinctive feature of δ_{CP} compared to the other PMNS parameters. As shown in Fig. 3, where the QFI and classical Fisher information (FI) are evaluated for the mixing angle θ_{13}, flavor measurements are optimal or nearly optimal at the oscillation maximum. In contrast, for δ_{CP}, a substantially larger and persistent gap between QFI and FI is observed across the parameter range, highlighting its fundamentally reduced information accessibility in flavor measurements (more details on the other PMNS parameters can be found in [31]). The strategy centered around the first oscillation maximum is strongly suboptimal, yielding FI values that are several orders of magnitude smaller than the corresponding QFI. In contrast, around the second oscillation maximum the FI is typically enhanced, in agreement with earlier analyses [39], which pointed out that the second peak amplifies the relative dependence of the appearance probability on δ_{CP}. This observation suggests that experiments targeting the second oscillation maximum, such as ESSνSB, are intrinsically better suited for the determination of δ_{CP} than first-peak setups like T2K or T2HK, unless the latter can achieve substantially higher statistics.

A closer inspection of Fig. 2, however, reveals that this amplification depends sensitively on the actual value of δ_{CP}. For example, in the case of maximal CP violation, $\delta_{CP} = \pi/2$, the FI decouples from the oscillation probability and exhibits oscillations with approximately twice the frequency: it is strongly suppressed at the second oscillation peak and instead reaches its maximum between probability minima and maxima. Nonetheless, larger overall values of $F_{\nu,\bar{\nu}}(\delta_{CP})$ are still attained at peaks corresponding to higher values of L/E. This indicates that achieving the corresponding estimation precision requires a more careful experimental design, going beyond a simple analysis based solely on probability oscillations. This is illustrated in Fig. 4, where the effective FI is shown as a function of δ_{CP} for three representative choices of L/E: the first and second oscillation peaks, and the value maximizing the FI over the first two periods. While the second peak generally yields higher FI than the first, this enhancement is significant only at large δ_{CP}, particularly near $\delta_{CP} = \delta_{CP}^{(\mathrm{NO})}$, and is strongly reduced around $\delta_{CP} = \pi/2$, where the maximum shifts away from the peaks.

These features highlight potential "information blind spots" in fixed-beam configurations. Tunable setups—such as off-axis sampling (e.g., DUNE-PRISM) or adjustable magnetic horns—can mitigate this limitation by enabling a dynamic optimization of the neutrino flux. For ESSνSB, for instance, a fixed baseline favors a spectrum peaked around 200 MeV, with further improvement near 300 MeV.

On the optimal measurement for δ_{CP} estimation—QET allows us to identify an optimal measurement such that the corresponding FI saturates the QFI. This measurement corresponds to the projection onto the eigenstates of the

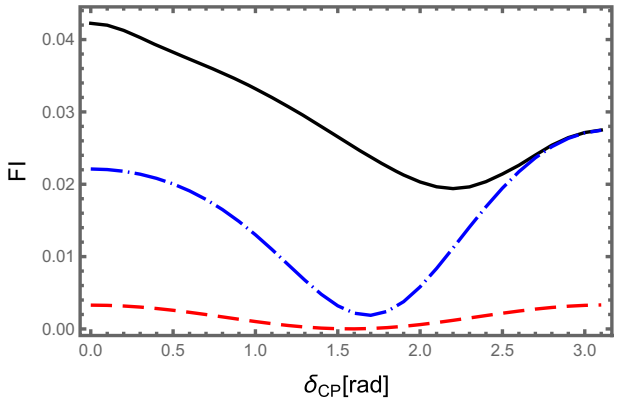


FIG. 4. The effective FI vs δ_{CP} for three representative L/E values. Black solid line: optimized over the first two oscillation periods; red dashed line: first oscillation peak taken in correspondence of the peak energy and baseline of T2K/T2HK ($L/E \approx 490$ km/GeV); blue dash-dotted line: second oscillation peak taken in correspondence of the peak energy and baseline of ESSνSB ($L/E \approx 1440$ km/GeV). The FI are plotted over the interval $[0, \pi]$, since the results are symmetric with respect to π, and the corresponding values over $[\pi, 2\pi]$ are obtained by reflection.

symmetric logarithmic derivative (SLD) operator L_λ, which for pure-state statistical models $|\psi_\lambda\rangle$ takes the explicit form [11]

$$L_\lambda = 2(|\partial_\lambda \psi_\lambda\rangle\langle\psi_\lambda| + |\psi_\lambda\rangle\langle\partial_\lambda \psi_\lambda|). \tag{9}$$

As is apparent from this expression, the SLD operator is defined primarily on the two-dimensional "informational" subspace $\mathcal{S} = \text{span}\{|\psi_\lambda\rangle, |\partial_\lambda \psi_\lambda\rangle\}$. In this pure-state scenario, the optimal measurement is not unique; one can prove that any projective measurement corresponding to a rotation of the eigenstates of L_λ within $\mathcal{S}$ is optimal [40], and thus for example the one including a projection on $|\psi_\lambda\rangle$. Furthermore, since the orthogonal complement $\mathcal{S}^\perp$ contains no information regarding the parameter, one can always identify a locally optimal "on/off" measurement characterized by the projectors $\Pi_{\text{on}} = |\psi_\lambda\rangle\langle\psi_\lambda|$ and $\Pi_{\text{off}} = \mathbb{I} - \Pi_{\text{on}}$.

Regarding the estimation of the CP-violating phase δ_{CP}, the optimal measurement corresponding to the eigenstates of the SLD operator $L_{\delta_{CP}}$ generally requires a projection onto a superposition of flavor eigenstates. In particular the mathematically optimal "on/off" measurement discussed above only coincides with a standard flavor measurement if the evolved neutrino state $|\nu_\alpha(t)\rangle$ aligns with a flavor eigenstate. This occurs only when the neutrino oscillates back into its initial flavor, the disappearance channel. However, at these specific points, the state's sensitivity to the phase vanishes, leading to a vanishing QFI, and thus also to a vanishing FI. This confirms the well-known result that the disappearance channel is fundamentally insensitive to δ_{CP}, and that the information instead resides in the interference terms accessible only via the appearance channels or non-flavor-diagonal measurements.

Conclusions—We applied QET to study the estimation of δ_{CP} via neutrino oscillations experiments, computing both the corresponding QFI and classical FI, in order to assess whether the current experimental uncertainty is limited by the information encoded in the neutrino quantum state itself or by the restriction to flavor measurements, which constitute the only feasible detection strategy. The QFI is insensitive to δ_{CP} and follows the oscillation pattern of the appearance probability. The corresponding Cramér-Rao bound yields $\sigma \sim 3°$, roughly an order of magnitude smaller than the current best-fit value [1], indicating that present uncertainties are not limited by the information encoded in the neutrino quantum state. Instead, we find that the restriction to flavor measurements constitutes a limiting factor for the achievable precision. The FI varies with δ_{CP} and grows at higher-order oscillation maxima, revealing enhanced sensitivity at the second and third peaks. At the first maximum, where current experiments operate, the FI is orders of magnitude below the QFI, underscoring the suboptimal nature of flavor measurement strategies. The planned ESSνSB experiment, targeting the second peak, achieves a FI approaching the QFI, demonstrating near-optimal extraction of the available quantum information. Although the largest limitation to the precision originates from the measurement strategy rather than the quantum state itself, it should still be regarded as an intrinsic impediment at the first oscillation peak, unless a substantial increase in statistics becomes feasible. Building on the present results, an upcoming paper will compute the QFI and FI for additional neutrino oscillation parameters, providing a unified framework to compare their respective sensitivities [31]. This Letter, part of the growing effort to connect high-energy physics with quantum information theory and quantum sensing [41–43], provides a quantitative foundation for optimizing future neutrino oscillation experiments. Our analysis shows that achieving precise δ_{CP} measurements does not require fundamentally new quantum states, but rather a strategic experimental configuration, specifically, targeting higher oscillation maxima, that maximizes the extraction of existing information.

Although our Letter is primarily focused on the foundational aspects of the quantum metrology applied to neutrino physics, our results provide a fundamental, model-independent benchmark for the precision achievable by current and future experiments. By deriving the Cramér-Rao bound in an ideal scenario (assuming perfect detector efficiency and no matter effects), we provide a hard limit. A violation of this bound in a proposed experiment would indicate a flaw in design or a biased estimator. Having such ultimate limits is a crucial tool for the quantification of such bias. Furthermore, our framework acts as a diagnostic tool for prioritizing experimental upgrades. While this Letter establishes the ideal scenario, the formalism is designed to

incorporate experimental imperfections, in a systematic and relatively simple way. This will allow experimentalists to quantify exactly how specific factors (such as detector inefficiencies, matter effects, and nonmonochromatic spectra) degrade the FI relative to the ultimate quantum bound. Consequently, our approach has the potential to guide the community on where to focus: it will allow us to identify which specific experimental limitations are the primary bottlenecks preventing the saturation of the quantum limit. More generally, QET thus emerges as a powerful tool for benchmarking and guiding experimental design in high energy physics, shifting the focus from sheer statistics to strategic information use.

Acknowledgments—The authors acknowledge insightful discussions with D. Alves, P. Coloma, and A. Serafini, and in particular thank F. Terranova for his valuable help and stimulating discussions.

Data availability—There are no publicly available research data or software supporting this manuscript. Requests for further information or data should be sent to the authors.

[1] I. Esteban, M. C. Gonzalez-Garcia, M. Maltoni, I. Martinez-Soler, J. P. Pinheiro, and T. Schwetz, J. High Energy Phys. 12 (2024) 216.
[2] K. Abe *et al.*, Eur. Phys. J. C **83**, 782 (2023).
[3] M. A. Acero, P. Adamson, L. Aliaga, N. Anfimov, A. Black *et al.* (The NOνA Collaboration), Phys. Rev. D **106**, 032004 (2022).
[4] DUNE Collaboration, arXiv:1512.06148.
[5] F. Terranova, Universe **10**, 221 (2024).
[6] M. Yokoyama, J. High Energy Phys. 08 (2023) 101.
[7] M. Singh, M. Bustamante, and S. K. Agarwalla, arXiv:2305.05184.
[8] A. Alekou *et al.*, Universe **9**, 347 (2023).
[9] A. Alekou *et al.*, Eur. Phys. J. C **81**, 1130 (2021).
[10] S. Davidson, E. Nardi, and Y. Nir, Phys. Rep. **466**, 105 (2008).
[11] M. G. A. Paris, Int. J. Quantum. Inf. **07**, 125 (2009).
[12] C. W. Helstrom, J. Stat. Phys. **1**, 231 (1969).
[13] V. Giovannetti, S. Lloyd, and L. Maccone, Nat. Photonics **5**, 222 (2011).
[14] C. L. Degen, F. Reinhard, and P. Cappellaro, Rev. Mod. Phys. **89**, 035002 (2017).
[15] L. Pezzè, A. Smerzi, M. K. Oberthaler, R. Schmied, and P. Treutlein, Rev. Mod. Phys. **90**, 035005 (2018).
[16] F. Albarelli, M. Barbieri, M. Genoni, and I. Gianani, Phys. Lett. A **384**, 126311 (2020).
[17] V. Montenegro, C. Mukhopadhyay, R. Yousefjani, S. Sarkar, U. Mishra, M. G. Paris, and A. Bayat, Phys. Rep. **1134**, 1 (2025),
[18] D. Bak, Phys. Lett. B **756**, 200 (2016).
[19] N. Lashkari and M. Van Raamsdonk, J. High Energy Phys. 04 (2016) 153.
[20] A. Trivella, Classical Quantum Gravity **34**, 105003 (2017).
[21] S. Banerjee, J. Erdmenger, and D. Sarkar, J. High Energy Phys. 08 (2018) 001.
[22] C. Gómez and R. Jimenez, Phys. Rev. D **102**, 063511 (2020).
[23] J. Erdmenger, K. T. Grosvenor, and R. Jefferson, SciPost Phys. **8**, 073 (2020).
[24] C. Gómez and R. Jimenez, J. Cosmol. Astropart. Phys. 09 (2021) 016.
[25] J. Feng and J.-J. Zhang, Phys. Lett. B **827**, 136992 (2022).
[26] A. Candeloro, C. Degli Esposti Boschi, and M. G. A. Paris, Phys. Rev. D **102**, 056012 (2020).
[27] L. Seveso and M. G. A. Paris, Ann. Phys. (Amsterdam) **380**, 213 (2017).
[28] C. Cepollaro, F. Giacomini, and M. G. A. Paris, Quantum **7**, 946 (2023).
[29] P. Asenov, W. Zhang, and A. Serafini, Phys. Rev. D **113**, 016015 (2026).
[30] M. Piotrak, T. Colas, A. Alonso-Serrano, and A. Serafini, J. High Energy Phys. 02 (2026) 199.
[31] C. Frugiuele, M. G. Genoni, M. Ignoti, and M. G. A. Paris, J. High Energy Phys. 08 (2026) 218.
[32] E. K. Akhmedov and A. Y. Smirnov, Phys. At. Nucl. **72**, 1363 (2009).
[33] S. Eliezer and A. R. Swift, Nucl. Phys. **B105**, 45 (1976).
[34] S. M. Bilenky and B. Pontecorvo, Lett. Nuovo Cimento **17**, 569 (1976).
[35] H. Fritzsch and P. Minkowski, Phys. Lett. **62B**, 72 (1976).
[36] K. Abe *et al.* (T2K Collaboration), Nucl. Instrum. Methods Phys. Res., Sect. A **659**, 106 (2011).
[37] K. Abe, N. Abgrall, H. Aihara, T. Akiri, J. B. Albert, C. Andreopoulos *et al.* (T2K Collaboration), Phys. Rev. D **87**, 012001 (2013).
[38] A. Alekou, E. Baussan, A. K. Bhattacharyya, N. Blaskovic Kraljevic *et al.*, Eur. Phys. J. Special Topics **231**, 3779 (2022).
[39] P. Coloma and E. Fernandez-Martinez, J. High Energy Phys. 04 (2012) 089.
[40] A. Fujiwara and H. Nagaoka, Phys. Lett. A **201**, 119 (1995).
[41] A. Chou *et al.*, arXiv:2311.01930.
[42] C. Beadle, H. Bekker, D. Blas, D. Budker, S. Calatroni, R. T. D'Agnolo, A. Dıaz-Morcillo, S. A. R. Ellis, C. Gatti, I. Garcıa-Irastorza, B. Gimeno, D. F. J. Kimball, N. Koss, A. Macpherson, W. L. Millar, K. Peters, A. O. Sushkov, A. Wickenbrock, J. Walter, and Y. Zhang, Quantum sensing for dark matter and gravitational waves, Technical Report, 2026, https://cds.cern.ch/record/2933206.
[43] Y. Afik *et al.*, Eur. Phys. J. Plus **140**, 855 (2025).

End Matter

Neutrino oscillations—Neutrino oscillations in vacuum are a quantum mechanical phenomenon made possible by the existence of nondegenerate neutrino masses (m_1, m_2, m_3) and lepton flavor mixing. The origin of flavor

mixing in the lepton sector lies in the mismatch between the orthonormal basis of interacting flavor eigenstates ($|\nu_e\rangle, |\nu_\mu\rangle, |\nu_\tau\rangle$) and the orthonormal basis of mass eigenstates ($|\nu_1\rangle, |\nu_2\rangle, |\nu_3\rangle$).

The unitary transformation relating the left-handed flavor eigentstate neutrino fields to the left-handed mass eigenstate neutrino fields is the Pontecorvo-Maki-Nakagawa-Sakata (PMNS) matrix:

$$\begin{pmatrix} \nu_e(x) \\ \nu_\mu(x) \\ \nu_\tau(x) \end{pmatrix}_L = \begin{pmatrix} U_{e1}U_{e2}U_{e3} \\ U_{\mu1}U_{\mu2}U_{\mu3} \\ U_{\tau1}U_{\tau2}U_{\tau3} \end{pmatrix} \begin{pmatrix} \nu_1(x) \\ \nu_2(x) \\ \nu_3(x) \end{pmatrix}_L . \tag{A1}$$

Considering neutrinos as Dirac fermions, the PMNS matrix can be parametrized by three mixing angles (θ_{12}, θ_{13}, θ_{23}) and one CP-violating phase δ_{CP}. The explicit form of the PMNS matrix is

$$U = \begin{pmatrix} \cos\theta_{12}\cos\theta_{13} & \sin\theta_{12}\cos\theta_{13} & e^{-i\delta_{CP}}\sin\theta_{13} \\ -\sin\theta_{12}\cos\theta_{23} - e^{i\delta_{CP}}\cos\theta_{12}\sin\theta_{13}\sin\theta_{23} & \cos\theta_{12}\cos\theta_{23} - e^{i\delta_{CP}}\sin\theta_{12}\sin\theta_{13}\sin\theta_{23} & \cos\theta_{13}\sin\theta_{23} \\ \sin\theta_{12}\sin\theta_{23} - e^{i\delta_{CP}}\cos\theta_{12}\sin\theta_{13}\cos\theta_{23} & -\cos\theta_{12}\sin\theta_{23} - e^{i\delta_{CP}}\sin\theta_{12}\sin\theta_{13}\cos\theta_{23} & \cos\theta_{13}\cos\theta_{23} \end{pmatrix}. \tag{A2}$$

In the case in which neutrinos are Majorana fermions two additional phases appear but they do not affect oscillation probabilities.

From Eq. (A1), considering the quantum excitations of the fields—i.e., the quantum state of the particles—we can write

$$|\nu_\alpha\rangle = \sum_i U^*_{\alpha i}|\nu_i\rangle \quad \text{with} \quad \alpha = e, \mu, \tau, \tag{A3}$$

where $|\nu_i\rangle$ denotes the mass eigenstate with eigenvalue m_i.

In vacuum, each mass eigenstate $|\nu_i\rangle$ is an eigenstate of the free Hamiltonian with eigenvalue $E_i = \sqrt{p^2 + m_i^2}$, where p is the momentum of the neutrino beam, which without loss of generality is assumed to be identical for all mass eigenstates:

$$|\nu_i(t)\rangle = e^{-iE_i t}|\nu_i\rangle, \tag{A4}$$

thus propagation modifies the original coherent superposition in Eq. (A3), which is no longer a pure flavor eigenstate. Assuming that the neutrino is generated at time $t_0 = 0$ in a flavor eigenstate $|\nu_\alpha\rangle$, the neutrino state at a generic time t can be written as

$$|\nu_\alpha(t)\rangle = \sum_i U^*_{\alpha i} e^{-iE_i t}|\nu_i\rangle = \sum_i U^*_{\alpha i} e^{-iE_i t} \sum_\beta U_{\beta i}|\nu_\beta\rangle, \tag{A5}$$

where we have rewritten the evolved state in the flavor eigenbasis since in this Letter we are interested in flavor measurements. From this expression we observe that the neutrino state at time t depends on the parameters of the PMNS matrix, as well as on E_i and t.

The probability that at time t the neutrino of flavor α has oscillated into a neutrino of flavor β is given by

$$P(|\nu_\alpha\rangle \to |\nu_\beta\rangle) = |\langle\nu_\beta|\nu_\alpha(t)\rangle|^2 = \left|\sum_i U_{\beta i}U^*_{\alpha i}e^{-iE_i t}\right|^2. \tag{A6}$$

Since neutrinos are ultrarelativistic, the approximation $E_i \approx p + m_i^2/2E$ with $E \approx p$ is valid and the probability can be rewritten as

$$P(|\nu_\alpha\rangle \to |\nu_\beta\rangle) = \sum_{i,j} U_{\beta i}U^*_{\alpha i}U^*_{\beta j}U_{\alpha j}e^{i\frac{\Delta m^2_{ji}L}{2E}}, \tag{A7}$$

where $\Delta m^2_{ij} \equiv m_j^2 - m_i^2$ and $L \approx ct$. Thus the oscillation probability depends on the PMNS parameters, on the squared mass differences Δm^2_{ij}, and on the ratio L/E between the distance traveled by the neutrino and its energy. In experiments L is referred to as the baseline, i.e., the distance between the production and detection points of the neutrino beam.

Expanding Eq. (A7) we obtain

$$P(|\nu_\alpha\rangle \to |\nu_\beta\rangle) = \delta_{\alpha\beta} - 4\sum_{i<j}\mathrm{Re}[U_{\alpha i}U^*_{\beta i}U^*_{\alpha j}U_{\beta j}]\sin^2\left(\frac{\Delta m^2_{ji}L}{4E}\right) + 2\sum_{i<j}\mathrm{Im}[U_{\alpha i}U^*_{\beta i}U^*_{\alpha j}U_{\beta j}]\sin\left(\frac{\Delta m^2_{ji}L}{2E}\right). \tag{A8}$$

We can clearly see that the term "neutrino oscillations" is used since the probability of flavor changing is a sum of sinusoidal and sine squared functions of the variable L/E. Moreover we observe that the phase δ_{CP} enters through the imaginary parts of the PMNS matrix combinations.

On the properties of the QFI—In the Letter we mentioned that we observe no strong dependence of

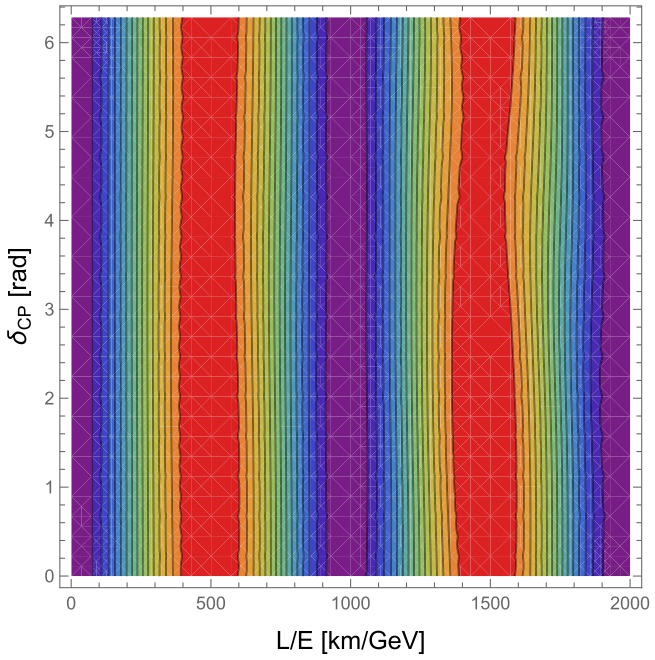


FIG. 5. Contour plot showing the dependence of the QFI $H_\nu(\delta_{CP})$ on the value of δ_{CP} and on the value of L/E. Analogous plot is obtained for $H_{\bar{\nu}}(\delta_{CP})$.

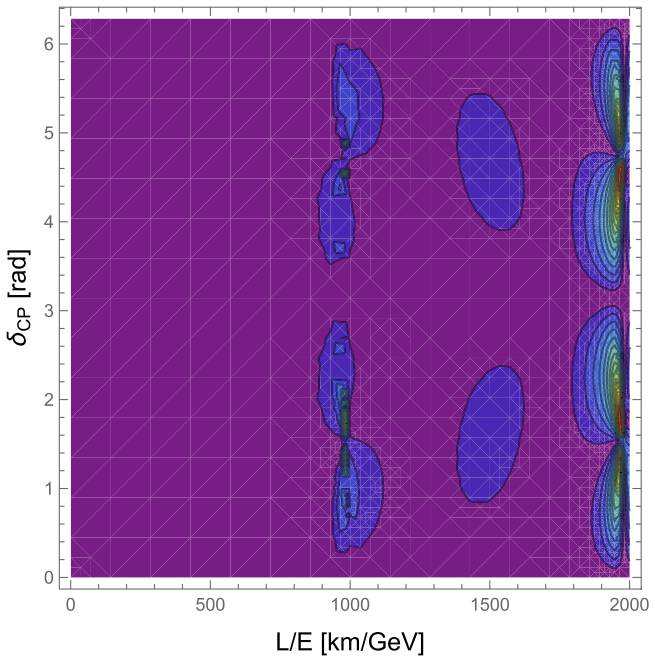


FIG. 6. Relative difference of $H_{\nu,\bar{\nu}}$ as a function of δ_{CP} and L/E. The relative difference is of the order or below 5% for almost all parameter space. The peaks in the relative difference are due to the smallness of the QFI in those region rather than on an actual significant difference in the QFIs.

$H_{\nu,\bar{\nu}}(\delta_{CP})$ on the value of δ_{CP}. In order to justify this claim, in Fig. 5 we plot the values of $H_\nu(\delta_{CP})$ as a function of δ_{CP} and of L/E, with the other parameters evaluated at the NuFIT best-fit values. We can clearly see that for fixed value of L/E, the QFI shows little to no dependence on the value of δ_{CP}. In the Letter, we also affirm that within the parameter regime of interest the quantum Fisher information for neutrinos and anti-neutrinos satisfies $H_\nu(\delta_{CP}) \simeq H_{\bar{\nu}}(\delta_{CP})$. The validity of this claim is shown in Fig. 6, where we show the relative difference of these two quantities $\Delta_{\nu,\bar{\nu}} = 2|H_\nu - H_{\bar{\nu}}|/(H_\nu + H_{\bar{\nu}})$ as a function of δ_{CP} and L/E. In the region of interest, corresponding to the oscillation peaks, this difference is at the level or below $O(1 \times 10^{-1})$ and is thus not significant, particularly in view of the small absolute value of the QFI (see Fig. 5).